Vol 16 No 2, February 2007
1009-1963/2007/16(02)/0429-06

Chinese Physics

© 2007 Chin. Phys. Soc.
and IOP Publishing Ltd

Enhancement of Kerr nonlinearity with vanishing absorption in a tripod scheme*

Sun Hui(孙 辉), Niu Yue-Ping(钮月萍), and Gong Shang-Qing(龚尚庆)†

State Key Laboratory of High Field Laser Physics, Shanghai Institute of Optics and Fine Mechanics, Chinese Academy of Sciences, Shanghai, 201800, *China*

(Received 11 February 2006; revised manuscript received 1 September 2006)

The giant enhancement of Kerr nonlinearity in a four-level tripod type system is investigated theoretically. By tuning the value of the Rabi frequency of the coherent control field, owing to the double dark resonances, the giant-enhanced Kerr nonlinearity can be achieved within the right transparency window. The influence of Doppler broadening is also discussed.

Keywords: Kerr nonlinearity, dark resonance, transparency window, Doppler broadening
PACC: 4250

1. Introduction

There are many interesting phenomena in quantum optics and atomic physics, induced by quantum coherence and interference. Examples include electromagnetically induced transparency (EIT),[1−5] coherent population trapping or transfer (CPT)[6,7] and lasing without inversion (LWI).[8−12] In nonlinear optics,[13] the third-order Kerr nonlinearity $\chi^{(3)}$ plays an important role, and the enhanced Kerr nonlinearity has some useful applications in cross-phase modulation[14] and self-phase modulation for the generation of optical solitons.[15] In a multi-level atomic system with EIT, nonlinear optical processes, such as four-wave mixing[16−18] and frequency conversion[19] can be greatly enhanced. It is desirable to realize the giant Kerr nonlinearity with low light powers,[20−22] since it can be used to realize single-photon nonlinear devices. In recent years, both theoretically[23−26] and experimentally,[27−30] tremendous interest has been aroused in the study of large third-order nonlinear susceptibility with reduced, especially with vanishing, linear absorption. In Ref.[23], Matsko *et al*, based on multilevel atomic coherence, proposed a new method of resonant enhancement of Kerr nonlinearity where one-photon resonant absorption is suppressed by coherence effects. By use of autoionizing resonance, the third-order nonlinearities can be enhanced while the absorption is cancelled.[24] Considering the interaction of dark resonances,[31] the Kerr nonlinearity can be enhanced several orders of magnitude accompanied by vanishing linear absorption.[25]

In this paper, enlightened by the work in Refs.[25] and [32], the enhancement of Kerr nonlinearity in a four-level tripod atomic system is studied theoretically. As pointed out in Ref.[32], there are two transparency windows, and changing the value of the Rabi frequency of the coherent-control field will lead to an asymmetric spectrum. This is different from that in Ref.[31], where the asymmetric spectrum was achieved by tuning the detuning of the coherent-control field. In this atomic system, the magnitude of Kerr nonlinearity can be enhanced several orders within the right transparency window by appropriately choosing the value of the Rabi frequency of the coherent-control field due to the double dark resonances. The enhancement is achieved by the presence of the coherent-control field, since it can induce the quantum coherence of the lower states. At the end of this paper, the influence of Doppler broadening[33] is discussed.

2. Model and basic equations

The conserved atomic system, i.e. there is no decay to states outside this system, considered in this

*Project supported by the National Natural Science Foundation of China (Grant No 60478002) and the Key Basic Research Foundation of Shanghai (Grant Nos 04JC14036 and 05DJ14003).
†E-mail: sqgong@mail.siom.ac.cn

paper is the same as that in Ref.[32] and is shown in Fig.1, which can exhibit double electromagnetically induced transparencies. Three lower states $|b\rangle$, $|c\rangle$, and $|d\rangle$ are coupled near-resonantly to the excited state $|a\rangle$ by the probe, the pump and the coherent-control fields, with carrier frequencies ν_1, ν_2, and ν_3, respectively; γ_1, γ_2, and γ_3 denote the population relaxation decay rates from the excited state $|a\rangle$ to the lower states $|b\rangle$, $|c\rangle$, and $|d\rangle$, respectively. Within the rotating wave approximation, the full set of density matrix equations are given by

$$\dot{\rho}_{aa} = -\mathrm{i}(g^*\rho_{ab} - g\rho_{ba}) - \mathrm{i}(G^*\rho_{ac} - G\rho_{ca}) - \mathrm{i}(\Omega^*\rho_{ad} - \Omega\rho_{da}) - (\gamma_1+\gamma_2+\gamma_3)\rho_{aa}, \tag{1}$$

$$\dot{\rho}_{bb} = \mathrm{i}(g^*\rho_{ab} - g\rho_{ba}) + \gamma_1\rho_{aa}, \tag{2}$$

$$\dot{\rho}_{cc} = \mathrm{i}(G^*\rho_{ac} - G\rho_{ca}) + \gamma_2\rho_{aa}, \tag{3}$$

$$\dot{\rho}_{dd} = \mathrm{i}(\Omega^*\rho_{ad} - \Omega\rho_{da}) + \gamma_3\rho_{aa}, \tag{4}$$

$$\dot{\rho}_{ac} = \mathrm{i}\Delta_0\rho_{ac} + \mathrm{i}g\rho_{bc} + \mathrm{i}G(\rho_{cc} - \rho_{aa}) + \mathrm{i}\Omega\rho_{dc} - \frac{\gamma_1+\gamma_2+\gamma_3}{2}\rho_{ac}, \tag{5}$$

$$\dot{\rho}_{ad} = \mathrm{i}\Delta_\mathrm{c}\rho_{ad} + \mathrm{i}g\rho_{bd} + \mathrm{i}G\rho_{cd} + \mathrm{i}\Omega(\rho_{dd} - \rho_{aa}) - \frac{\gamma_1+\gamma_2+\gamma_3}{2}\rho_{ad}, \tag{6}$$

$$\dot{\rho}_{ab} = \mathrm{i}\Delta\rho_{ab} + \mathrm{i}g(\rho_{bb} - \rho_{aa}) + \mathrm{i}G\rho_{cb} + \mathrm{i}\Omega\rho_{db} - \frac{\gamma_1+\gamma_2+\gamma_3}{2}\rho_{ab}, \tag{7}$$

$$\dot{\rho}_{cd} = \mathrm{i}(\Delta_\mathrm{c} - \Delta_0)\rho_{cd} + \mathrm{i}G^*\rho_{ad} - \mathrm{i}\Omega\rho_{ca}, \tag{8}$$

$$\dot{\rho}_{cb} = \mathrm{i}(\Delta - \Delta_0)\rho_{cb} - \mathrm{i}g\rho_{ca} + \mathrm{i}G^*\rho_{ab}, \tag{9}$$

$$\dot{\rho}_{db} = \mathrm{i}(\Delta - \Delta_\mathrm{c})\rho_{db} - \mathrm{i}g\rho_{da} + \mathrm{i}\Omega^*\rho_{ab}. \tag{10}$$

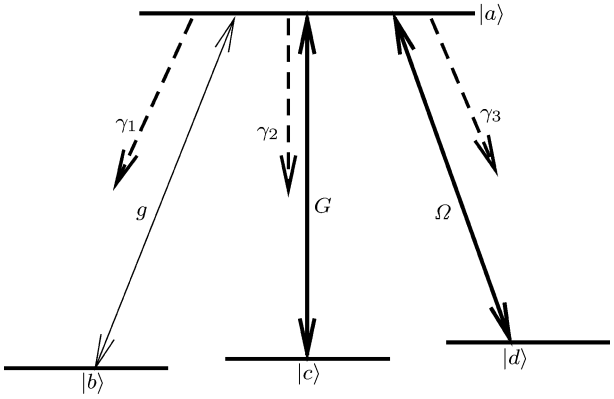


Fig.1. Schematic diagram of energy levels for a four-level tripod system studied. It consists of three lower states and an excited state, denoted by $|b\rangle$, $|c\rangle$, $|d\rangle$, and $|a\rangle$, respectively. The three lower states are respectively coupled to the excited state via the probe, the pump and the coherent-control fields.

The above equations are constrained by $\sum_i \rho_{ii} = 1$ and $\rho_{ij} = \rho^*_{ji}$, $(i, j = a,\ b,\ c\ ,d,$ and $i \neq j)$. Here Δ, Δ_0, and Δ_c are the detunings of the probe, the pump and the coherent-control fields respectively. They are defined as $\Delta = \omega_{ab} - \nu_1$, $\Delta_0 = \omega_{ac} - \nu_2$, and $\Delta_\mathrm{c} = \omega_{ad} - \nu_3$. In the simplified case, the dephasing rates between states $|b\rangle$, $|c\rangle$, and $|d\rangle$ are not included. Furthermore, the strengths of the atom-field coupling are given by the Rabi frequencies $g = \boldsymbol{\mu}_{ba}\cdot\boldsymbol{E}_1/\hbar$ on the $|b\rangle \leftrightarrow |a\rangle$ transition, $G = \boldsymbol{\mu}_{ca}\cdot\boldsymbol{E}_2/\hbar$ on the $|c\rangle \leftrightarrow |a\rangle$ transition, and $\Omega = \boldsymbol{\mu}_{da}\cdot\boldsymbol{E}_3/\hbar$ on the $|d\rangle \leftrightarrow |a\rangle$ transition, where $\boldsymbol{\mu}_{ba}$, $\boldsymbol{\mu}_{ca}$, and $\boldsymbol{\mu}_{da}$ denote the electric dipole matrix elements.

3. Results and discussions

The third-order nonlinear susceptibility is the parameter for special consideration. By taking $\rho^{(0)}_{bb} = 1.0$ and assuming that the intensity of the probe field is very small as compared with those of the pump and the coherent-control fields, $\rho^{(1)}_{ab}$ and $\rho^{(3)}_{ab}$ can be solved in the steady state. By combining with $\chi = \chi^{(1)} + 3|E_1|^2\chi^{(3)}$, the linear susceptibility $\chi^{(1)}$ and the third-order nonlinear susceptibility $\chi^{(3)}$ are given by

$$\chi^{(1)} = -\frac{2N|\boldsymbol{\mu}_{ab}|^2}{\hbar\varepsilon_0\mathcal{Z}}[(\Delta - \Delta_0)(\Delta - \Delta_\mathrm{c})], \tag{11}$$

$$\chi^{(3)} = \frac{2N|\boldsymbol{\mu}_{ab}|^4}{3\hbar^3\varepsilon_0 g\mathcal{Q}}\left(\mathcal{A}\mathrm{Re}[\rho_{db}^{(1)}] + \mathcal{B}\mathrm{Im}[\rho_{db}^{(1)}] + \mathcal{C}\mathrm{Re}[\rho_{cb}^{(1)}] + \mathcal{D}\mathrm{Im}[\rho_{cb}^{(1)}] + \mathcal{F}\mathrm{Im}[\rho_{ab}^{(1)}]\right), \tag{12}$$

where

$$\mathcal{Z} = [\Delta + \mathrm{i}(\gamma_1+\gamma_2+\gamma_3)/2](\Delta-\Delta_0)(\Delta-\Delta_\mathrm{c}) - G^2(\Delta-\Delta_\mathrm{c}) - \Omega^2(\Delta-\Delta_0). \tag{13}$$

Here $\mathcal{A}$, $\mathcal{B}$, $\mathcal{C}$, $\mathcal{D}$, $\mathcal{F}$, $\mathcal{Q}$ are functions of G, Ω, Δ, Δ_0, Δ_c, γ_q $(q = 1, 2, 3)$, (their explicit expressions are so complicated that they will not be presented here), and N is the atom density.

For the sake of convenience, all parameters are reduced to dimensionless ones by scaling with γ_1. Considering the case when $\Delta_0 = -1.0$, $\Delta_\mathrm{c} = 1.0$, the variations of the refractive part of the third-order nonlinear susceptibility (solid curve) and the imaginary part of the linear susceptibility $\mathrm{Im}[\chi^{(1)}]$ (dashed curve) versus the probe detuning Δ with different intensities of the coherent-control field are plotted in Fig.2. For brevity, the effect due to the different value of the population decay from the excited state $|a\rangle$ to different ground state sublevels $|i\rangle$ $(i = b, c, d)$ is not considered. Parameters are taken to be $\gamma_2 = \gamma_3 = 1.0$, $G = 1.0$, (a) $\Omega = 1.0$, (b) $\Omega = 0.2$. The magnitude of $\mathrm{Im}[\chi^{(1)}]$ in Fig.2(b) is magnified 10 times for the sake of clarity, and the inset shows the behaviour within the right transparency window. In agreement with that demonstrated in Ref.[32], it can be obtained from Fig.2(a) that there are two transparency windows, whose positions are determined by Δ_0 and Δ_c, namely, the positions of the two transparency windows can be shifted by changing Δ_0 or Δ_c. This can also be derived from Eq.(11). The real part of $\chi^{(3)}$ is symmetric around the two transparency windows, however it has also a strong linear absorption. This is undesirable for application. Fortunately, we can get around this by changing the value of Rabi frequency of the coherent-control field Ω, since it can cause the refractive part of $\chi^{(3)}$ to be asymmetric. By comparing the case when $\Omega = 0.2$ with that in Fig.2(a), one can find that the magnitude of the real part of $\chi^{(3)}$ is increased about one order. More important is that, by decreasing the Rabi frequency of the coherent-control field, the large real part of $\chi^{(3)}$ is shifted into the right transparency window, i.e. with vanishing linear absorption. This can be seen more clearly from the inset. This is desirable for the application of it.

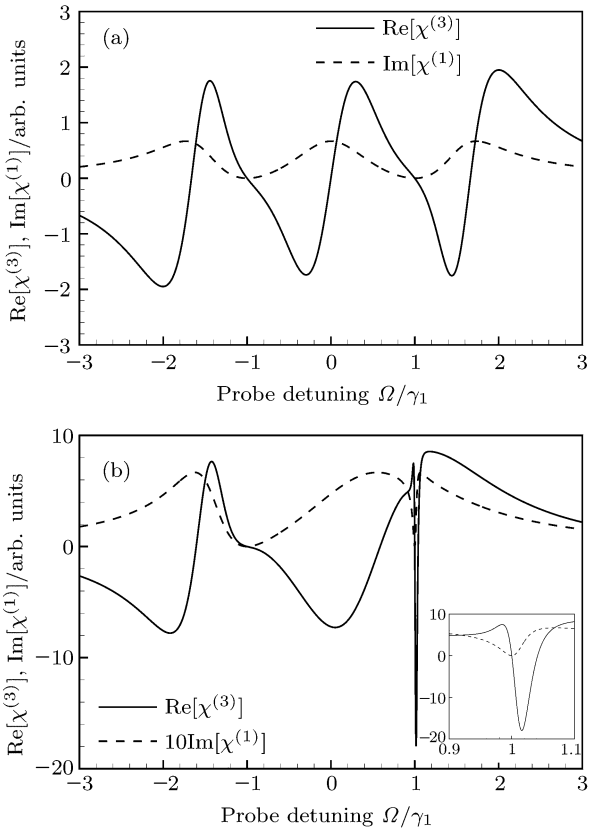


Fig.2. Variations of $\mathrm{Re}[\chi^{(3)}]$ (solid) and $\mathrm{Im}[\chi^{(1)}]$ (dashed) versus the probe detuning Δ. The common parameters are taken to be $\gamma_2 = \gamma_3 = 1.0$, $\Delta_0 = -1.0$, $\Delta_\mathrm{c} = 1.0$, $G = 1.0$, (a) $\Omega = 1.0$, (b) $\Omega = 0.2$. In (b), $\mathrm{Im}[\chi^{(1)}]$ is magnified 10 times for clarity. The inset illustrates the behaviour in the vicinity of the right transparency window.

It is instructive to compare the enhanced Kerr nonlinearity with that in a three-level Λ type system and to consider the influence of the detuning of the pump field and the intensity of the coherent-control field, because they can change the absorption property correspondingly. The variations of $\mathrm{Re}[\chi^{(3)}]$ in the presence (solid curve) and absence of the coherent-control field (long-dashed curve) and $\mathrm{Im}[\chi^{(1)}]$ (dashed curve) versus the probe detuning Δ are plotted in Fig.3. The parameters are $\gamma_2 = \gamma_3 = 1.0$, $\Delta_0 = 0.0$, $\Delta_\mathrm{c} = 1.0$, $G = 1.0$, (a) $\Omega = 0.2$, (b) $\Omega = 0.1$. In Figs.3(a) and (b), $\mathrm{Im}[\chi^{(1)}]$ are magnified 10 and 20 times, respectively. In comparison with the solid and

long-dashed curves in Fig.3(a), the magnitude of the real part of $\chi^{(3)}$ is much larger than that in a three-level Λ type system. From Figs.2(b) to 3(a), one can find that the enhanced $\mathrm{Re}[\chi^{(3)}]$ within the right transparency window is varied from asymmetric to symmetric. By reducing the value of Rabi frequency of the coherent-control field to $\Omega = 0.1$ (see Fig.3(b)), the magnitude of Kerr nonlinearity can be increased much more.

Next, we investigate the physical mechanism leading to giant enhancement of Kerr nonlinearity. Considering the case $\gamma_2 = \gamma_3 = 1.0$ and $\Delta_0 = 0.0$ for convenience, we have $\mathcal{A}$, $\mathcal{B}$, $\mathcal{C}$, $\mathcal{D}$, $\mathcal{F}$, $\mathcal{Q}$ in Eq.(12) as follows:

$$
\begin{aligned}
\mathcal{A} &= [2\Delta(\Delta-\Delta_{\mathrm{c}})]/\Omega,\\
\mathcal{B} &= -\frac{4\Delta}{3\Omega\Delta_{\mathrm{c}}}[(\Delta-\Delta_{\mathrm{c}})(G^2-\Delta_{\mathrm{c}}^2)+\Omega^2(\Delta-2\Delta_{\mathrm{c}})],\\
\mathcal{C} &= [2\Delta(\Delta-\Delta_{\mathrm{c}})]/G,\\
\mathcal{D} &= \frac{4(\Delta-\Delta_{\mathrm{c}})}{3G\Delta_{\mathrm{c}}}[\Delta(G^2+\Omega^2)+G^2\Delta_{\mathrm{c}}],\\
\mathcal{F} &= \frac{1}{3G^2\Omega^2\Delta_{\mathrm{c}}^2}\{(\Delta-\Delta_{\mathrm{c}})[8\Delta\Delta_{\mathrm{c}}^2G^4-9\Delta\Delta_{\mathrm{c}}^2(G^2+\Omega^2)-4\Delta\Delta_{\mathrm{c}}^4G^2-4\Delta(G^2+\Omega^2)^3]\\
&\quad -\Delta_{\mathrm{c}}^2[4\Delta(10\Delta-9\Delta_{\mathrm{c}})G^2\Omega^2-4G^2\Omega^2(G^2+\Omega^2)+6\mathrm{i}(2\Delta-\Delta_{\mathrm{c}})G^2\Omega^2]\},\\
\mathcal{Q} &= (\Delta-\Delta_{\mathrm{c}})(2G^2-2\Delta^2-3\mathrm{i}\Delta)-2\Delta\Omega^2.
\end{aligned}
$$

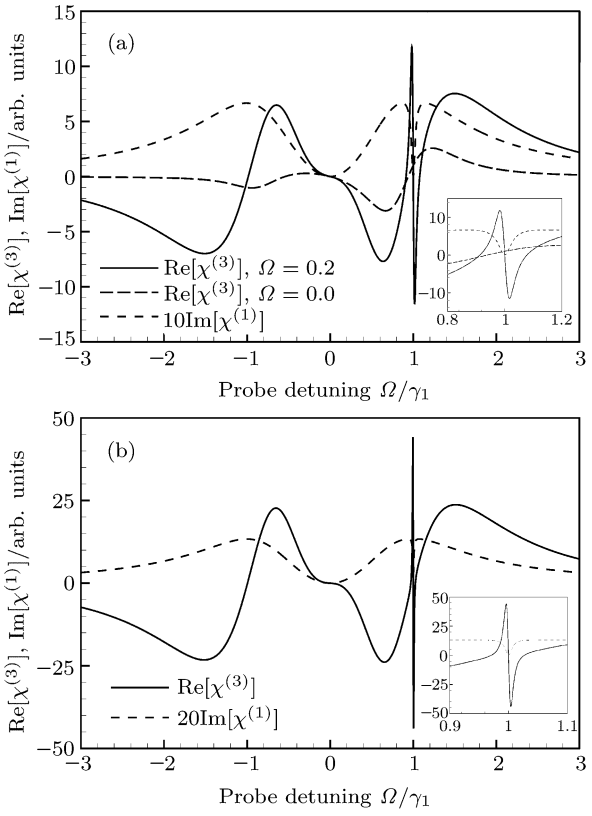


Fig.3. Variations of $\mathrm{Re}[\chi^{(3)}]$ with (solid curve) and without the coherent-control field (long-dashed curve) and $\mathrm{Im}[\chi^{(1)}]$ (dashed curve) versus the probe detuning Δ. Parameters are $\gamma_2 = \gamma_3 = 1.0$, $\Delta_0 = 0.0$, $\Delta_{\mathrm{c}} = 1.0$, $G = 1.0$, (a) $\Omega = 0.2$, (b) $\Omega = 0.1$. The insets show the behaviour in the vicinity of the right transparency window.

Equation (12) exhibits that there are five major contributions to the third-order nonlinear susceptibility. In order to make their influence more clearly, in Figs.4(a) and 4(b), $\mathrm{Re}[\chi^{(3)}]$ and their contributions versus the probe detuning Δ are plotted, respectively. The inset in Fig.4(b) demonstrates the behaviour within the right transparency window, and the contribution from $\mathrm{Im}[\rho_{db}^{1}]$ is magnified 1.5 times for clarity. The parameters are the same as those in Fig.3(b). Figure 4(a) shows that, in the region beyond the right transparency window, Kerr nonlinearity (dashed curve) is influenced dominantly by one-photon resonant absorption (solid curve), and the contributions of the other four terms are very small. However, within the right transparency window, the contribution from $\mathrm{Im}[\rho_{ab}^{(1)}]$ is reduced dramatically. The enhanced giant refractive part of $\chi^{(3)}$ is mainly attributed to the quantum coherence of states $|b\rangle$ and $|d\rangle$, and it is induced by the coherent-control field, which can be seen clearly from Eqs.(14) and (15). Equations (14)-(17) show that, when the value of the Rabi frequency of the coherent-control field is much smaller than that of the pump field, $\mathcal{A}, \mathcal{B} \gg \mathcal{C}, \mathcal{D}$, the contributions from $\rho_{cb}^{(1)}$ are very small, and can be ignored.

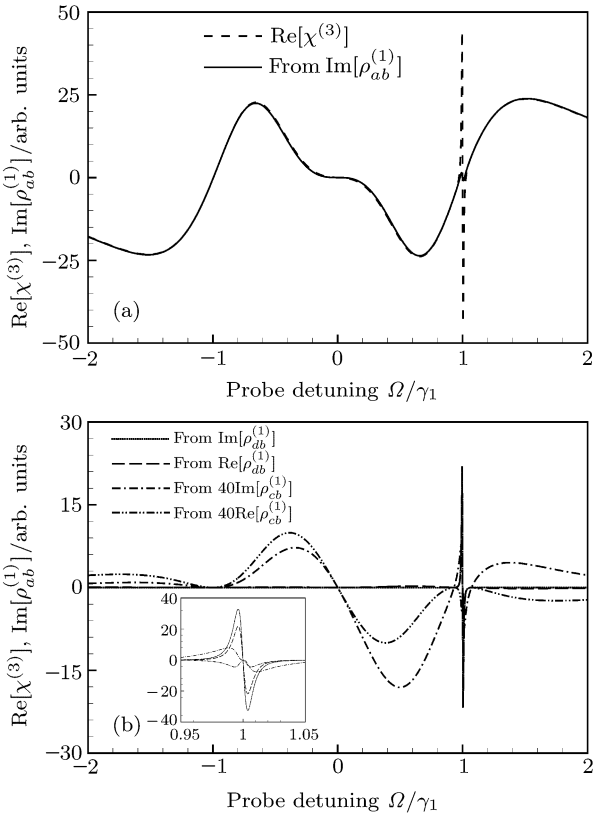


Fig.4. Re[$\chi^{(3)}$] ((a) dashed) and the contributions from Im[$\rho_{ab}^{(1)}$]) ((a) solid), Im[$\rho_{db}^{(1)}$] ((b) dotted), Re[$\rho_{db}^{(1)}$] ((b) long-dashed), Im[$\rho_{cb}^{(1)}$] ((b) dot-dashed), Re[$\rho_{cb}^{(1)}$] ((b) double dot-dashed) versus the probe detuning Δ. The parameters are the same as those in Fig.3(b). The inset shows the behaviour in the vicinity of the transparency window. For clarity, the magnitude of the contribution from Im[$\rho_{db}^{(1)}$] is magnified 1.5 times.

4. Doppler broadening

The above treatment ignores the effect of Doppler broadening. In practice, the atoms may move with a velocity v, giving an effective frequency for the probe, the pump and the coherent-control fields of $\nu_1 - k_1 v$, $\nu_2 - k_2 v$, and $\nu_3 - k_3 v$ due to the Doppler effect, where $k_{1,2,3} = \pm\nu_{1,2,3}/c$ with $+(-)$ indicating that the probe, the pump and the control fields propagate in the same (opposite) direction of the atom motion. For the sake of simplicity, we assume $k_1 = k_2 = k_3 = k$ and the probe, the pump and the coherent-control fields propagate in the same direction of the atom motion. By using $\nu_1 \to \nu_1 - kv$, $\nu_2 \to \nu_2 - kv$, $\nu_3 \to \nu_3 - kv$, and integrating over the Maxwell–Boltzmann distribution for velocities, the third-order nonlinear susceptibility is then given by

$$\chi^{(3)} = \int_{-\infty}^{\infty} \chi^{(3)}(v) f(kv) \mathrm{d}(kv), \qquad (14)$$

where

$$f(kv)\mathrm{d}(kv) = \frac{1}{\sqrt{2\pi\delta^2}} \exp(-k^2 v^2/2\delta^2)\mathrm{d}(kv); \qquad (15)$$

and

$$\delta = \sqrt{k_B T \nu_1^2 / Mc^2}, \qquad (16)$$

is a measure of the Doppler width in the Maxwell–Boltzmann distribution.

Figure 5 shows the variation of the refractive part of the third-order nonlinear susceptibility versus the probe detuning Δ with different Doppler broadenings: $\delta = 0.0$ (solid curve), $\delta = 0.2$ (double dot-dashed curve), and $\delta = 1.5$ (dashed curve). The parameters are the same as those in Fig.3(b). The result when $\delta = 0.2$ (double dot-dashed curve) shows that the refractive part of the third-order nonlinear susceptibility is not sensitive to Doppler broadening because the Doppler width is much smaller than the Rabi frequency ($G = 1.0$) of the pump field. However, for large Doppler width, it is no longer the case. For intensity, when $\delta = 1.5$, the magnitude of the refractive part of the third-order susceptibility is dramatically reduced. It can be understood that the quantum coherence is weakened because of Doppler broadening. In order to overcome the influence of the decoherence due to Doppler broadening, we can choose cold atoms to obtain the giant enhancement.

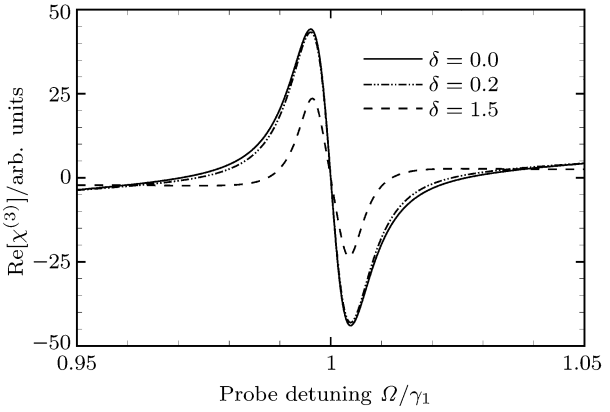


Fig.5. Variations of Re[$\chi^{(3)}$] versus the probe detuning Δ with different Doppler broadenings: $\delta = 0.0$ (solid curve), $\delta = 0.2$ (double dot-dashed curve), and $\delta = 1.5$ (dashed curve). Parameters are the same as those in Fig.3(b).

5. Conclusions

In conclusion, the possibility of enhancing the Kerr nonlinearity based on double dark resonances in the four-level tripod system has been investigated. Owing to the double dark resonances, the Kerr nonlinearity can be enhanced several orders of magnitude

with vanishing linear absorption at a certain detuning by choosing the value of the Rabi frequency of the coherent-control field appropriately. This is due to the presence of the coherent-control field, which can induce the quantum coherent of states $|b\rangle$ and $|d\rangle$. In principle, the magnitude of Kerr nonlinearity can be enhanced much more by decreasing the intensity of the coherent-control field. Beyond this window, the one-photon resonant absorption is dominantly responsible for the Kerr nonlinearity. The contributions from the quantum coherence of the states $|b\rangle$ and $|c\rangle$ are very small and can be ignored because the value of Rabi frequency of the coherent-control field is chosen much smaller than that of the pump field.

References

[1] Harris S E 1997 *Phys. Today* **52** 36

[2] Boller K J, Imamoğlu A and Harris S E 1991 *Phys. Rev. Lett.* **66** 2593

[3] Marangos J P 1998 *J. Mod. Opt.* **45** 471

[4] Gea-Banacloche J, Li Y Q, Jin S Z and Xiao M 1995 *Phys. Rev. A* **51** 576

[5] Li Y Q and Xiao M 1995 *Phys. Rev.* A **51** R2703

[6] Scully M O and Zubairy M S 1997 *Quantum Optics* (Cambridge University Press, Cambridge)

[7] Bergmann K, Theuer H and Shore B W 1998 *Rev. Mod. Phys.* **70** 1003

[8] Harris S E 1989 *Phys. Rev. Lett.* **62** 1033

[9] Imamoğlu A and Harris S E 1989 *Opt. Lett.* **14** 1344

[10] Gong S Q, Teng H G and Xu Z Z 1995 *Phys. Rev.* A **51** 3382

[11] Popov A K, Myslivets S A, Gao J Y, Zhang H Z and Wellegehausen B 2000 *Chin. Phys.* **9** 124

[12] Zhang B, Xu W H, Zhang H F and Gao J Y 2004 *Chin. Phys.* **13** 1721

[13] Boyd R W 1992 *Nonlinear Optics* (Academic, San Diego, Calif.)

[14] Schmidt H and Imamoğlu A 1996 *Opt. Lett.* **21** 1936

[15] Tikhonenko Vladimir, Christou Jason and Luther-Davies Barry 1996 *Phys. Rev. Lett.* **76** 2698

[16] Li Y Q and Xiao M 1998 *Opt. Lett.* **21** 1064

[17] Merriam A J, Sharpe S J, Shverdin M, Manuszak D, Yin G Y and Harris S E 2000 *Phys. Rev. Lett.* **84** 5308

[18] Li J H, Yang W X and Peng J C 2004 *Chin. Phys.* **13** 1694

[19] Harris S E, Field J E and Imamoğlu A 1990 *Phys. Rev. Lett.* **64** 1107.

[20] Harris S E and Hau L V 1999 *Phys. Rev. Lett.* **82** 4611

[21] Imamoğlu A, Schmidt H, Woods G and Deutsch M 1997 *Phys. Rev. Lett.* **79** 1467

[22] Hemmer P R, Katz D P, Donoghue J, Cronin-Golomb M, Shahriar M S and Kumar P 1995 *Opt. Lett.* **20** 982

[23] Matsko A B, Novikova I, Welch G R and Zubairy M S 2003 *Opt. Lett.* **28** 96

[24] Nakajima Takashi 2000 *Opt. Lett.* **25** 847

[25] Niu Y P, Li R X, Gong S Q and Liang X Y *Opt. Lett.* **30** 3371

[26] Hong Tao, Jack Michael Wong, Yamashita Makoto and Mukai Takaaki 2002 *Opt. Commun.* **214** 271

[27] Wang Hai, Goorskey Dabid and Xiao Min 2001 *Phys. Rev. Lett.* **87** 073601

[28] Wang Hai, Goorskey Dabid and Xiao M 2002 *Phys. Rev.* A **65** 051802(R)

[29] Wang Hai, Goorskey Dabid and Xiao M 2002 *J. Mod. Opt.* **49** 335

[30] Akulshin A M, Sidorov A I, McLean R J and Hannaford P 2004 *J. Opt.* B: *Quantum Semiclass. Opt.* **6** 491

[31] Lukin M D, Yelin S F, Fleischhauer M and Scully M O 1999 *Phys. Rev. A* **60** 3225

[32] Paspalakis E and Knight P L 2002 *J. Opt.* B: *Quantum Semiclass. Opt.* **4** S372

[33] Sun H, Guo H, Bai Y F, Han D A, Fan S L and Chen X Z 2005 *Phys. Lett.* A **335** 68